

## SPECIAL ISSUE ARTICLE

# The desertification process in the Silk Road Economic Belt in the past 15 years: A study using MODIS data and GIS analysis

Xiaofeng Wang<sup>1,2,3,4</sup>  | Lichang Yin<sup>1</sup> | Feiyan Xiao<sup>1</sup> | Mingming Zhang<sup>1</sup> | Lili Liu<sup>1</sup> | Zixiang Zhou<sup>5</sup> | Yong Ao<sup>1</sup>

<sup>1</sup>The School of Earth Science and Resources, Chang'an University, Xi'an, China

<sup>2</sup>State Key Laboratory of Urban and Regional Ecology, Research Center for Eco-Environmental Sciences, Chinese Academy of Sciences, Beijing, China

<sup>3</sup>The School of Land Engineering, Chang'an University, Xi'an, China

<sup>4</sup>Key Laboratory of Degraded and Unused Land Consolidation, The Ministry of Land and Resources of China (Shaanxi Provincial Land Engineering Construction Group, Co. Ltd), Xi'an, China

<sup>5</sup>College of Geomatics, Xi'an University of Science and Technology, Xi'an, China

## Correspondence

Xiaofeng Wang, The School of Earth Science and Resources, Chang'an University, Xi'an, 710054, China.

Email: wangxf@chd.edu.cn

## Funding information

National Natural Science Foundation of China, Grant/Award Number: 4104011; High Performance Demonstration System of Earth Surface System for Scientific Research and Application, Grant/Award Number: 30-Y30B13-9003-14/16; Fundamental Research Funds for the Central Universities, Grant/Award Number: 310827162026; Shaanxi Province Foundation of Important Science & Technology Innovative Team, Grant/Award Number: 2016KCT-23

Handling Editor: R. Li

The arid region in the northern part of China is a bridge between China and neighbouring countries in the Silk Road Economic Belt, and the severe desertification in this region restricts its sustainable development. In this paper, MODIS data, including albedo, reflectance, normalized vegetation index, and land surface temperature, were selected in 2000, 2005, 2010, and 2015 to construct a decision tree to extract spatio-temporal information of the desertified land in the arid area. The trend in desertification and transfer directions was analysed by the GIS method, and the dynamic characteristics of the desertification at different units (provincial administrative unit and typical sandy land) and with different topographic factors (slope and aspect) are discussed. Our conclusions include (a) desertification in the arid region in the northern part of China showed improvement overall and local deterioration. The deteriorating areas were located primarily in the western region of the Hunshandake Sandy Land, the tectonic zone of the Taklimakan Desert, and the Qaidam Basin; (b) the degree of desertification transfer occurred primarily at adjacent levels; (c) the desertified area in each province showed a different trend in fluctuation, and Maowusu Sandy Land recovered better among the 4 large sands; and (d) the desertified area was distributed primarily along 0°–3° slopes and showed a rapid decline at increased slopes. The change in the degree of desertification in each aspect largely was a general reversal, and the area of the north aspect was larger than that of other areas of aspects. This study provides some theoretical support for the control of desertification in the Silk Road Economic Belt.

## KEYWORDS

desertification, GIS, MODIS, the Silk Road Economic Belt

## 1 | INTRODUCTION

China is promoting an infrastructure development agenda actively in the Silk Road Economic Belt, with the goal of promoting regional and subregional economic development (Tracy, Shvarts, Simonov, & Babenko, 2017). The Silk Road Economic Belt stretches across Asia, Europe, and Africa (Li, Qian, Ken, Howard, & Wu, 2015b), including 65 core countries, and accounts for 41.3% of the total area of the world (Li et al., 2014). It cannot achieve rapid economic development without the construction of the modern ecological civilization (Li et al., 2016). However, the ecological environment is fragile along the Silk Road, especially midway through the second Asia–Europe

continental bridge, where there is less vegetation and serious desertification (Li et al., 2014). The rapid expansion of this desertification degrades the environment, leads to huge economic losses, and poses a threat to human survival and development (Armah et al., 2011; Reynolds et al., 2011). Therefore, neighbouring countries must work together to address these problems (Ren & Tang, 2015). The arid region of the northern part of China is located midway through the second Asia–Europe continental bridge. Its desertification is self-evident and is the principal constraint on regional ecological environment and the sustainable development of the social economy (Wang, Zhu, & Wu, 2002). As a result, desertification in the Silk Road Economic Belt must be prevented and controlled to construct the ecological

civilization. The study of desertification prevention and control in this arid region of the northern part of China can be used to provide a reference for countries in the Silk Road Economic Belt.

Monitoring and assessing desertification helps identify the dynamic characteristics of different degrees of desertification (Vogt et al., 2011) and has been an important method in the scientific prevention and control of desertification (Millennium Ecosystem Assessment Council, 2005). However, because of the dynamics and complexity of desertification, it is difficult to monitor it (Dawelbait & Morari, 2012; Eswaran, Lal, & Reich, 2001). Wide range remote sensing (RS) with large amounts of information has been used widely to monitor desertification (Barzani & Khairulmaini, 2013; Holm, Cridland, & Roderick, 2003; Nicholson, Tucker, & Ba, 1998; Sastry, Ganesha Raj, Paul, Dhinwa, & Sastry, 2016; Sepehr, Hassanli, Ekhtesasi, & Jamali, 2007). Tottrup and Rasmussen (2004) analysed grassland desertification in Senegal using NOAA/AVHRR NDVI data; Reiche et al. (2012) discovered the state of grassland desertification in Xilinguole using field survey data and ASTER images. Wang, Song, Yan, Li, and Jiali (2011) used Landsat MSS/TM/ETM RS data as their information source. Information about desertification in the northern part of China was extracted by visual interpretation, and the dynamic changes in its desertification from 1975 to 2010 were analysed. The results showed that the region of desertification development and reversal occurred primarily in the semiarid area of the agropastoral ecotone, and the key areas of desertification control were the ecotone between agriculture and animal husbandry in the eastern part of the northern part of China. Luo, Xu, and Ren (2013) selected MODIS data to construct a decision tree based on albedo, NDVI, and reflectance to extract Ordos sandy desertification, and their results showed that MODIS data reflected land desertification on the regional scale accurately. Meng et al. (2012) also based their study on MODIS data combined with albedo, LST, FVC, TVDI, and other indicators to establish a decision tree to extract information about the Hulunbeier Sandy Land with an accuracy of 89%. Compared with other satellite data, MODIS data with medium resolution have the characteristics of freeness, wide

coverage, high time resolution, and rich late product and are more suitable in monitoring desertification in the macroscopic range (Badreldin & Goossens, 2013; Zolotokrylin et al., 2016).

Therefore, 2000, 2005, 2010, and 2015 MODIS synthesis product data, including albedo, reflectance, the normalized vegetation index (NDVI), and land surface temperature (LST), were selected to build a decision tree to extract spatio-temporal information about the desertified land in the arid region of the northern part of China. Further, the spatio-temporal evolution of desertification over the past 15 years was analysed with the GIS spatial analysis technique to provide a theoretical basis for desertification control in the Silk Road Economic Belt.

## 2 | MATERIALS AND METHODS

### 2.1 | Study area

The arid area is a region with low precipitation and soil moisture content, which includes primarily arid, semiarid, and semihumid climate areas (Türkeş, 1999). The arid region in the northern part of China, one important part of the arid land in central Asia, is a seriously fragile ecological region (Yao et al., 2013) that lies between 36°44′–49°57′N and 73°26′–123°55′E. It includes the west of the Daxing'anling Mountains, the north of the Kunlun Mountains–Qilian Mountains, and the Great Wall line (Li, Zhao, Zhao, & Zhang, 2011b; Sun, Liu, & Lei, 2016). To ensure the integrity of the administrative boundary of the study area, six provinces (Xinjiang, Gansu, Qinghai, Ningxia, Shaanxi, and Inner Mongolia) comprised the study area (Figure 1). In this region, the main vegetation types are temperate grassland and desert, with poor natural conditions and rare precipitation. The desertification problem is very prominent here and includes eight deserts and four main sands.

### 2.2 | Data sources

The data sources used included (a) MOD09A1 8d (reflectance) and MCD43A3 8d (albedo) with a resolution of 500 m derived from USGS

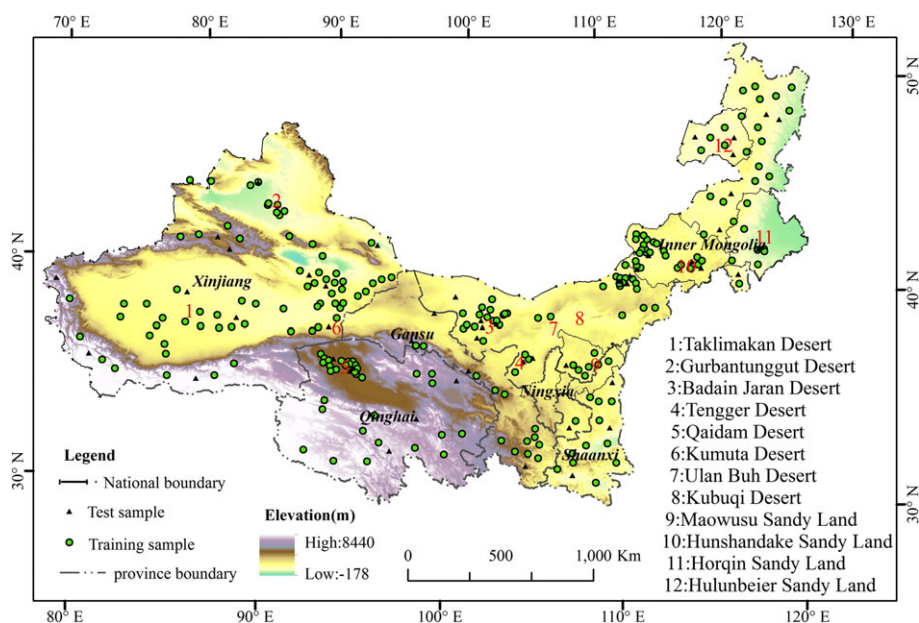


FIGURE 1 Map of the study area

(<https://lpdaac.usgs.gov>). The track numbers were h23v04, h23v05, h24v04, h24v05, h25v03, h25v04, h25v05, h26v03, h26v04, h26v05, h27v04, and h27v05; (b) MODND1M(NDVI) and MODLT1M(LST) monthly synthetic products (7, 8, and 9), with resolutions of 500 m and 1 km, were derived from the geospatial data cloud (<http://www.gscloud.cn>); and (c) DEM data with a resolution of 250 m came from the international scientific data service platform, the Chinese Academy of Sciences Computer Network Information Center.

Data preprocessing: the MRT software was used to mosaic and transform the project (convert SIN projection to Albers Equal Area and WGS84), convert the format (.hdf to .geotiff format), and resample (sampling mode for nearest neighbour, resolution of 500 m) the MODIS reflectance products (7th band) and albedo products (white sky band of 0.3 ~ 5  $\mu\text{m}$ ). The cell statistics tool in ArcGIS was used to maximize the reflectance and albedo data by month. A raster calculator was used to calculate the average layer of reflectance, albedo, NDVI, and LST for 7, 8, and 9 months. LST data were resampled to a resolution of 500 m. Four layers were fused to obtain single-layer multiband data in ENVI.

### 2.2.1 | Classification system

The selection of indices of the degree of desertification and the establishment of a classification system are the basis of desertification research (Hu, Dong, Lu, & Yan, 2011). This contributes to an objective and scientific understanding of the evaluation of the dynamic process of desertification (Luo et al., 2013). We selected NDVI, albedo, reflectance, and LST. NDVI reflects the vegetation growth status (Tucker et al., 2005), and the albedo reflects the surface energy balance (Schaaf et al., 2002). The reflectance and LST indicate surface dry and wet conditions (Sobrino, El Kharraz, & Li, 2003).

According to the existing desertification classification system (Li, Han, Xu, Ma, & Huang, 2006) and the actual situation in the study area, the degree of desertification was divided into very severe desertification (VS), severe desertification (S), moderate desertification (M), light desertification (L), and nondesertification (N). Shifting sandy land, Gobi

and wind erosion (residual hills) were assigned to VS, semifixed sand (mound) was assigned to S, bare sandy areas were assigned to M, and fixed sand (hill) was assigned to L.

### 2.2.2 | Decision tree construction

A decision tree is a mathematical method that summarizes training samples to generate decision trees or rules and then uses those rules to classify new data (Friedl & Brodley, 1997). Multisource RS data and a variety of indicators can be used fully to improve classification accuracy (Jia, Han, Lv, Wang, & Dongqi, 2011; Li, Liu, & Yuan, 2011a). The georeferencing tool in ArcGIS was used to match the distribution map of China's desertified land in 2014 with the study area vector boundary. According to the principle of representation and uniformity, 250 modelling points, including 200 training samples and 50 test samples, were selected. The value of each point of the four indicators was obtained by extracting multi values to point in ArcGIS. In general, the more serious desertification, the lower the vegetation coverage, NDVI smaller, on the contrary, the greater the albedo and reflectance (Zeng, Xiang, Feng, & Xu, 2006).

In this paper, we first analysed the relationship between LST, reflectance, and desertification. The training samples data showed that the LST values of VS, S, M and L are more than 7  $^{\circ}\text{C}$ , and the reflectance values are more than 2300, which can effectively divide the most part of N. For the other areas of the study area, the NDVI was as the main indicators of the redivision. Most of the NDVI of VS, including shifting sandy land, Gobi and wind erosion, was below 0.1, the small part was between 0.1 and 0.16, but the albedo of Gobi was less than 240. The NDVI values of S and M were between 0.1 and 0.3, with most of the former between 0.1 and 0.16, and most of the latter between 0.16–0.3. The NDVI values of L were primarily between 0.16 and 0.4. For the overlapped parts of NDVI, we again analysed the differences of albedo, reflectance, and LST to determine the threshold and constructed the decision tree (Figure 2). Then the model was constructed and run in ENVI, and the accuracy of the classification results

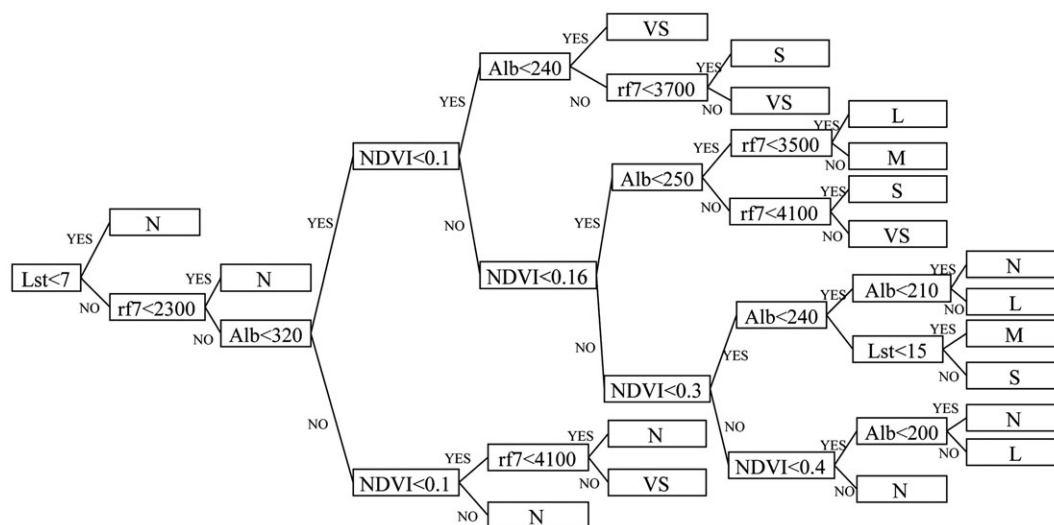


**FIGURE 2** Decision tree for extraction of information on desertification in the study area. Note: N denotes nondesertification, VS very serious desertification, S serious desertification, M medium desertification, and L light desertification. Lst denotes land surface temperature, rf7 reflectance, Alb albedo, and NDVI the normalized vegetation index

was verified. The Kappa coefficient was 0.86, which satisfied the research requirements. The final result was as follows.

The RS image classification accuracy test is an indispensable aspect of RS classification technology (Gan, Wang, Wang, & Fu, 1999). The Kappa coefficient Cohen (Cohen, 1968) proposed to evaluate the results of RS image classification has been used widely in classification (Luo et al., 2013). The calculation formula is as follows:

$$K = \frac{N \sum_{i=1}^n P_{ii} - \sum_{i=1}^n (P_{i+} * P_{+i})}{N^2 - \sum_{i=1}^n (P_{i+} * P_{+i})} \quad (1)$$

where  $K$  is the Kappa coefficient;  $P_{+i}$  and  $P_{i+}$  are the total number of pixels in the row and column of the  $i$  type, respectively;  $P_{ii}$  is the number of samples of the  $i$  type that are classified correctly;  $N$  is the total number of samples; and  $n$  is the number of types.

Different precision evaluation methods have different classification criteria and meanings. The Kappa coefficient classification criterion (Cicchetti & Feinstein, 1990; Feinstein & Cicchetti, 1990) is shown in Table 1.

The test samples in Figure 1 were imported in ENVI, and the Kappa coefficient was calculated using its confusion matrix function. The result showed that the Kappa coefficient was 0.86. So the consistency degree was optimal. This showed that the decision tree based on MODIS data and used to extract desertification information had a reasonable degree of reliability.

### 2.2.3 | GIS method

#### 1. Map analysis

Map analysis is among the ways to identify trends in desertification scientifically (Kang, Liu, & Duan, 2016). This paper first encoded the desertification land according to severity (Table 2).

Then we used the raster calculating tool in ArcGIS to obtain the dynamic data of different degrees of desertification. The calculation formula is as follows:

$$I = I_{k+1} - I_k, \quad (2)$$

where  $I$  is the code difference and  $I_{k+1}$  and  $I_k$  represent the  $k + 1$  and  $k$  period desertification degree codes, respectively.

**TABLE 1** Kappa coefficient classification criteria

Kappa	<0.0	0.0–0.2	0.2–0.4	0.4–0.6	0.6–0.8	0.8–1.0
Consistency degree	Very low	Weak	Mild	Medium	Significant	Optimal

**TABLE 2** Coding of degree of desertification

Code	1	2	3	4	5
Desertification degree	N	L	M	S	VS

Note. N = nondesertification; VS = very serious desertification; S = serious desertification; M = medium desertification; L = light desertification.

**TABLE 3** Classification of desertification trends

Classification criteria	$I > 2$	$1 \leq I \leq 2$	$I = 0$	$-2 \leq I \leq -1$	$I < -2$
Desertification trend	Obvious development	General development	Stability	General reversal	Obvious reversal

Finally, according to the value of  $I$ , desertification can be divided into different trends: obvious development, general development, stability, general reversal, and obvious reversal (Table 3).

#### 2. Desertification transfer matrix

A desertification transfer matrix is a better method to describe the mutual transformation between different degrees of desertification, as it reflects specifically the structural characteristics of desertification changes and the direction of the transfer between the various types (Duan, Wang, Xue, Xun, & Hai, 2013).

The general form of the desertification degree transfer matrix (Zhu & Li, 2003) is

$$C_{ij} = \begin{bmatrix} c_{11} & c_{12} & \cdots & c_{1n} \\ c_{21} & c_{22} & \cdots & c_{2n} \\ \cdots & \cdots & \cdots & \cdots \\ c_{n1} & c_{n2} & \cdots & c_{nn} \end{bmatrix}, \quad (3)$$

where  $C_{ij}$  represents the area of class  $i$  desertification during period  $k$  converted to the class  $j$  desertification in the  $k + 1$  period;  $n$  is the total type, and  $i, j$  ( $i, j = 1, 2, \dots, n$ ) represent the degree of desertification during the  $k$  and  $k + 1$  periods, respectively.

## 3 | RESULTS AND INTERPRETATION

### 3.1 | Dynamic change in desertification

From 2000 to 2015, the average area of desertification in the study area accounted for 36.7% of the total area, and thus, there was a desertification phenomenon in approximately one-third of the study area. The area of desertification had continued to decline from 157.18 million ha in 2000 to 147.36 million ha in 2015, a total reduction of 9.82 million ha (6.2%). The reduction occurred primarily in VS (Table 4).

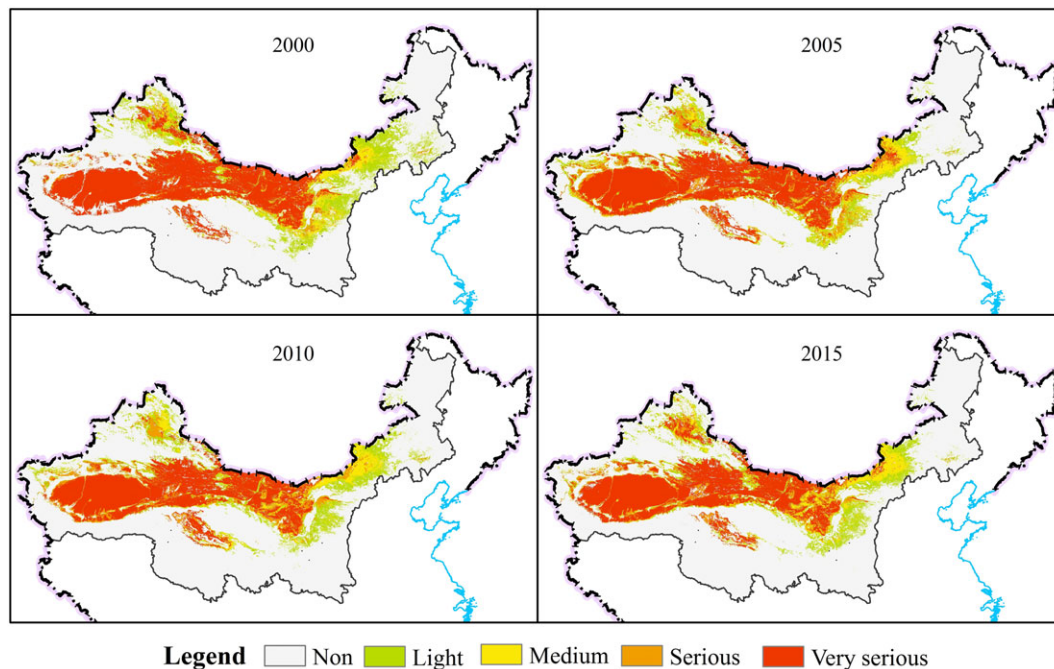
The different degrees of desertification, according to the size of their area were, in order: VS > L > S > M. VS accounted for more than 50% of the desertified area, which showed a continuous downward trend and a decrease of 13.12 million ha. L, S, and M areas showed different fluctuations. The amounts of change were –6.18 million ha, 7.32 million ha, and 2.16 million ha, respectively (Table 4).

From the perspective of the spatial distribution of desertification, VS was distributed primarily in the Taklimakan desert (TKLD), Badain Jaran desert (BDJD), Tengger desert (TGD), Ulan Buh desert (UBD), and the eastern part of Xinjiang. L was distributed primarily in the Horqin Sandy Land (HQSL), Maowusu Sandy Land (MWSSL), and Hunshandake Sandy Land (HSDKSL). The distribution of M was concentrated in the western region of HSDKSL, and S was distributed sporadically in the study area (Figure 3).

**TABLE 4** Desertification statistics in the study area from 2000 to 2015: unit: million ha

Desertification	2000	2005	2010	2015	2000–2005	2005–2010	2010–2015	2000–2015
L	37.76	28.15	34.23	31.58	–9.61	6.08	–2.66	–6.18
M	14.85	15.77	15.28	17.01	0.92	–0.48	1.72	2.16
S	11.67	22.86	23.30	19.00	11.19	0.44	–4.31	7.32
VS	92.89	88.85	77.58	79.78	–4.05	–11.26	2.20	–13.12
Total	157.18	155.63	150.40	147.36	–1.55	–5.23	–3.05	–9.82

Note. N = nondesertification; VS = very serious desertification; S = serious desertification; M = medium desertification; L = light desertification.

**FIGURE 3** Distribution of degree of desertification in the study area from 2000 to 2015

### 3.2 | Trends in desertification

During the past 15 years, the change in desertification was primarily stable, and the area of desertification reversal was larger than that of development. During 2000–2005, the area of desertification reversal was 40.68 million ha, with a general reversal rate of 84.63%. This was distributed primarily in the Gurbantunggut desert (GBTD), BDDJ, Kubuqi desert (KBQD), and HQSL. The area of desertification development was 35.32 million ha. The obvious development area was 33.7% and was concentrated in the TKLD edge. The general development area was concentrated in the HSDKSL (Table 5, Figure 4).

In 2005–2010, the area of desertification reversal was 43.86 million ha. The proportion of the general reversal area was 82.53%, mainly

**TABLE 5** Changes in desertification in the study area during 2000–2015: unit: million ha

Change	2000–2005a	2005–2010a	2010–2015a	2000–2015a
Obvious reversal	6.36	7.66	6.33	9.98
General reversal	34.32	36.20	22.76	44.28
Stability	339.74	353.21	357.71	334.91
General development	23.40	14.82	23.65	16.66
Obvious development	11.92	3.84	5.27	9.90

in the GBTD, the TKLD, and the HSDKSL. The area of desertification development was 18.66 million ha. The general development area was 79.4% and was concentrated in the HQSL and HSDKSL edge (Table 5, Figure 4).

In 2010–2015, the area of desertification reversal was slightly larger than was the development area, which was 29.99 million ha and 28.92 million ha, respectively. The general desertification development area was slightly larger than the general reversal area, 22.76 million ha and 23.65 million ha, respectively. The general reversal area was concentrated in the HSDKSL, whereas the general development area was distributed primarily in the GBTD and the south of the MWSSL (Table 5, Figure 4).

From 2000 to 2015, the area of reversal was approximately twice that of development, indicating that the overall trend of desertification in the study area has been curbed, although some areas are still deteriorating. The reversal in desertification was dominated by general reversal, with an area of 44.28 million ha (81.6%).

### 3.3 | Transfer matrix of desertification area

During the past 15 years, the transfer of desertification in the study area was concentrated in adjacent grades (Table 6). N shifted

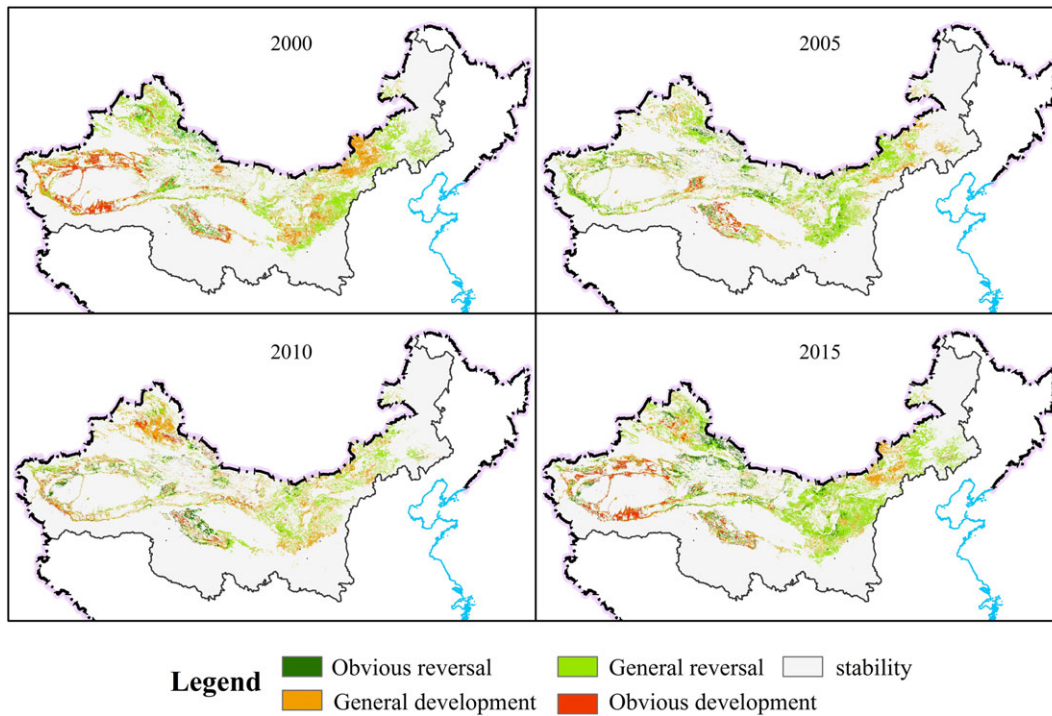


**FIGURE 4** Changes of desertification in study area during 2000–2015

**TABLE 6** Desertification area transfer in study area during 2000–2015: unit: million ha

Year range	Desertification degree	N	L	M	S	VS
2000–2005	N	235.97	8.92	2.8	5.23	6.09
	L	19.3	12.94	3.98	0.93	0.6
	M	0.73	3.29	6.17	3.07	1.59
	S	0.45	1.2	1.27	6.66	2.1
	VS	4.1	1.8	1.55	6.98	78.46
2005–2010	N	248.12	7.86	0.79	1.22	2.57
	L	11.39	14.37	1.06	1.13	0.21
	M	1.75	5.54	7.1	1.19	0.18
	S	2.19	3.1	3.02	11.43	3.12
	VS	2.33	3.36	3.31	8.34	71.51
2010–2015	N	252.26	9.2	0.78	1.3	2.23
	L	10.02	17.86	3.49	1.12	1.75
	M	1.49	2.01	8.79	1.41	1.58
	S	2.18	1.23	2.74	11.09	6.07
	VS	2.88	1.27	1.2	4.08	68.16

Note. N = nondesertification; VS = very serious desertification; S = serious desertification; M = medium desertification; L = light desertification.

primarily to L with an area of 8.41 million ha, accounting for 42.1% of the area transferred. L converted primarily to N, with a transfer area of 21.53 million ha, accounting for 85.5% of the area converted. M transferred primarily to L, with a transfer area of 4.9 million ha, accounting for 58.8% of the area converted. S converted primarily to VS, with an area of 2.01 million ha, and VS converted primarily to S, with an area of 8.49 million ha, accounting for 39.9% of the area converted. L, M, and VS shifted primarily to a lower degree of desertification, whereas N and M shifted primarily to a higher degree of desertification (Figure 5).

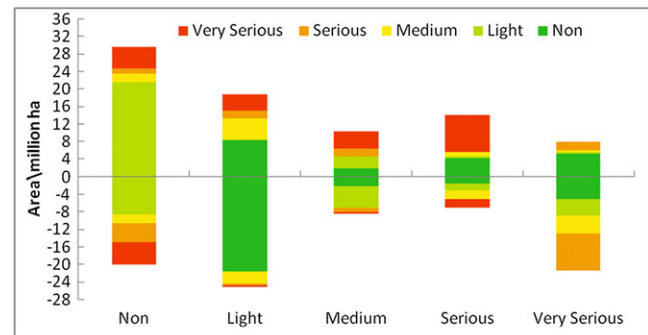


**FIGURE 5** Desertification area transfer in study area between 2000 and 2015. Note: Positive value indicates the value of transferring into and negative value indicates the value of transferring out

### 3.4 | Desertification change based on different units

#### 3.4.1 | Provincial administrative unit

According to the administrative boundaries of the provinces, this paper used a zoning statistical tool to obtain the deserted areas of the different provinces. Overall, the size of the deserted area was, from largest to smallest: Xinjiang, Inner Mongolia, Gansu, Qinghai, Ningxia, and Shaanxi. The average percents were 50.3%, 32.3%, 10.7%, 4.2%, 1.7%, and 0.7%, respectively. VS dominated in Xinjiang and Qinghai, S and M dominated in Inner Mongolia and Gansu, whereas L dominated in Ningxia and Shaanxi (Figure 6).

The change in the deserted areas in the six provinces differed. The deserted area in Qinghai and Xinjiang increased slightly, which was attributable primarily to S, whereas the deserted area in the other

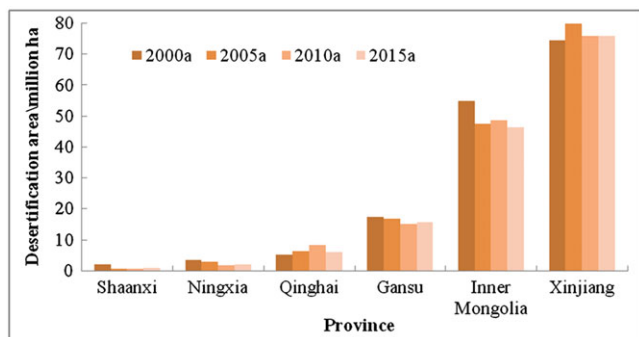


**FIGURE 6** Desertification area in six provinces

four provinces decreased. The reduced area of desertification in Shaanxi Province was mainly L and M, in Ningxia Province M and S, in Gansu Province VS, and in Inner Mongolia primarily VS and L (Table 7).

### 3.4.2 | Typical sandy land unit

The four main sands were typical sandy land in the study area, and the change in their degree of desertification affects the ecological and economic development of the surrounding areas. The HQLD border comes from Wang, Zhang, Ma, and Zhu (2016). The boundary of the HSDKSL is derived from Li, Meng, Bao, and Yin (2015a). The boundary of the MWSSL is derived from Hu et al. (2013). The HLBSL border comes from Bai (2013).

The changes in the degree of desertification in HLBSL, HSDKSL, and HQSL largely were stable, with a proportion of more than 60%, and in MWSSL, there was general reversal primarily. The general reversal ratio of each sandy land was higher than was the general development ratio. The proportion of obvious reversal also was greater than was the obvious development ratio. The difference between the proportion of reversal and development was highest in MWSSL, which indicated that it was recovering the best of the four main sands (Table 8).

## 3.5 | Desertification change based on topographic factors

Slope and aspect are important terrain factors that affect the erosion, handling, and accumulation of surface sand (Hu, Dong, Lu,

**TABLE 7** Change in areas of desertification and dominant type in six provinces

Province	2000–2005a	2005–2010a	2010–2015a	2000–2015a	Leading desertification degree
Shaanxi	–	–	+	–	L + M
Ningxia	–	–	–	–	M + S
Gansu	–	–	+	–	VS
Inner Mongolia	–	+	–	–	VS + L
Qinghai	+	+	–	+	S
Xinjiang	+	–	+	+	S

Note. VS = very serious desertification; S = serious desertification; M = medium desertification; L = light desertification. +/– represents an increase/decrease in desertification area.

**TABLE 8** Change in ratio of degree of desertification in typical sandy land in 2000–2015: unit: %

Sandy land type	General Stability	General reversal	General development	Obvious reversal	Obvious development
HLBSL	92.43	5.64	1.93	0.00	0.00
HSDKSL	60.60	23.53	15.70	0.15	0.02
HQSL	81.79	15.99	1.21	0.59	0.42
MWSSL	34.20	51.88	10.50	3.24	0.18

Note. HLBSL = Hulunbeier Sandy Land; HSDKSL = Hunshandake Sandy Land; HQSL = Horqin Sandy Land; MWSSL = Maowusu Sandy Land.

Song, & Zhenhai, 2010), and thus are important in the study of desertification.

### 3.5.1 | Slope

In this paper, we used the slope extraction function in ArcGIS to extract the slope from the DEM and divided it into six levels according to the existing desertification slope classification (Ma et al., 2010) and the slope condition of the study area.

From the distribution of the desertification slope, the desertified area showed a rapid decline with increased slope in 2000–2015. Desertification was distributed primarily among 0°–1° and 1°–3° slopes, with an average area of 94.21 million ha and 45.85 million ha, respectively (61.7% and 30.0%). They were dominated by VS. This was followed by the 3°–5° slope, with an average area of 7.3 million ha (4.8%) that was dominated by VS and L. The desertified area in other slopes was small and dominated by L (Table 9).

From the annual change rate of desertification at different slopes, 2005–2015a, 0°–15° of the annual change rate in desertification were negative and more than 15° of the annual change rate in desertification were positive. This indicated that below 15° of slope, the desertified area continued to decrease and above 15° of slope, the desertified area continued to increase.

### 3.5.2 | Aspect

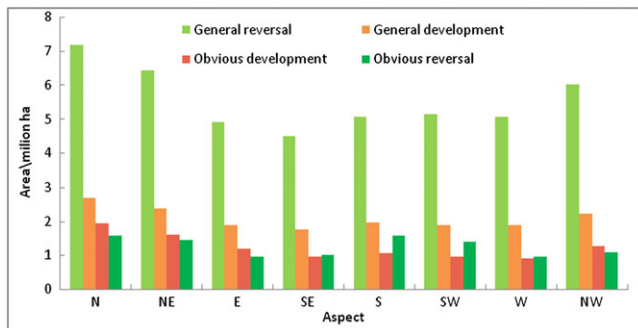
The aspect was extracted from the DEM of the six provinces in northern part of China using the slope extraction function in ArcGIS.

From 2000 to 2015, the area of general reversal of each aspect in the study area was the largest, and its average area was up to 5.53 million ha, among which, the area of general reversal in the north was the largest, at 7.18 million ha, whereas it was the lowest in the southeast, at 4.5 million ha. The areas of obvious development and obvious reversal were relatively less from 2000 to 2015, and in the south and southwest, the area of obvious reversal was significantly higher than was obvious development, and their areas were nearly the same, both in the west and southeast. However, in the north, northeast, east, and northwest, the area of obvious development was slightly higher than was obvious reversal (Figure 7).

Overall, the type of desertification in the study area at different aspects largely was general reversal from 2000 to 2015, with the order of area general reversal > general development > obvious development > obvious reversal in the north, northeast, east, and northwest, whereas the order was general reversal > general development >

**TABLE 9** Desertification changes at different slopes from 2000 to 2015

Slope range	Area (million ha)					Annual change rate of desertified area (%)		
	2000	2005	2010	2015	Average	2000–2005	2000–2010	2000–2015
0–1°	94.51	96.62	93.71	92.00	94.21	0.45	–0.08	–0.18
1–3°	48.84	45.84	45.01	43.72	45.85	–1.23	–0.78	–0.70
3–5°	8.27	7.28	6.85	6.79	7.30	–2.39	–1.72	–1.20
5–7°	2.83	2.55	2.21	2.26	2.46	–1.95	–2.17	–1.34
7–15°	2.24	2.51	2.03	1.98	2.19	2.37	–0.97	–0.78
>15°	0.42	0.78	0.58	0.60	0.60	17.62	3.91	2.98

**FIGURE 7** Change in trend in areas of desertification at different aspects from 2000 to 2015

obvious reversal > obvious development in the southeast, south, southwest, and west.

## 4 | DISCUSSION AND CONCLUSIONS

### 4.1 | Discussion

The decision tree based on MODIS data was used to calculate the desertification area of the study area in 2000, 2005, 2010, and 2015. They were 157.18 million ha, 155.63 million ha, 155.40 million ha, and 147.36 million ha, respectively. On the national scale, compared with the statistical data of China desertification (Tu, Li, & Sun, 2016), the errors of the classification area were 9.12%, 8.51%, 8.53%, and 3.26%, and the overall trend between the two is consistent. On the regional scale, the study of desertification in typical areas shows that the desertification area in HQSL continued to decrease from 2000 to 2010, which is consistent with the results of Duan et al. (2013) and Li et al. (2006) through interpretation of TM/ETM image. In the aspect of desertification change, Kang et al. (2016) used the MODIS data to construct the decision tree for analysing the desertification status in the central and western regions of Inner Mongolia and pointed out that the desertification of the MWSSL showed a stable reversal from 2000 to 2014 and the desertification of the HSDKSL was unstable. This study is in good agreement with that. In summary, the analytical method of this paper is suitable for desertification monitoring in the macroscopic range.

The driving factors of desertification land type change can be divided into natural factors and human factors. The average wind speed, temperature, and precipitation in natural factors have an

important influence on land desertification (Wang, Reng, & Ma, 2009). In the northern part of Xinjiang, there was a continuous warming in the past 15 years (Fang, Yue, Chen, & Sun, 2011), which accelerated the melting of glaciers and caused the growth of the vegetation in the area, inhibited the expansion of desertification and promoted the reversal of desertification. However, the rapid reduction of glacier and permanent snow is not conducive to the conservation of water resources and the sustainable development of ecological environment in regional socio-economic development (Liu, Xun, Dong, & Zhang, 2010). Human factors such as the implementation of a series of desertification control projects, including returning farmland to forest and grass, forbidden and forbidden logging, and the Three North Shelterbelt project, have resulted in effective control of desertification trends in MWSSL and HQSL (Kang et al., 2016; Wang et al., 2011). In further studies, the effects of precipitation, wind speed, wind direction, population, and land use on desertification in the study area can be quantitatively analysed by Geodetector (Wang & Xu, 2017) and other methods and provide scientific reference for ecological environment management.

### 4.2 | Conclusions

With the implementation of the Silk Road Economic Belt construction strategy, human activities in arid regions of the northern part of China will increase significantly (Li et al., 2014), and dynamic monitoring of desertification will become significantly more important. In this paper, we used MODIS data to construct a decision tree based on multiple indicators, and to extract information on desertification during the four periods. The precision was 85.6%, which indicated that the decision tree constructed in this manuscript was suitable for dynamic monitoring of desertification in the study area. We analysed the dynamic characteristics of desertification during the four periods in six provinces in the northern part of China by desertification map analysis and a desertification area transfer matrix. The results showed that (a) the overall desertification process in the arid region of the northern part of China is becoming better, but some areas are getting worse. The areas of deterioration were located primarily in the western region of HSDKSL, the tectonic zone of the TKLD, and the Qaidam Basin; (b) the degree of desertification transfer occurred largely at the adjacent level; (c) the desertified area of each province showed a different trend of fluctuation. Further, MWSSL recovered better among the four main sands; and (d) desertified areas were distributed primarily on 0°–3° slopes (~ 90%) and showed a rapid decline at increased slopes. The change in the degree of desertification for each slope primarily was

general reversal, and the area of the north aspect was larger than were the areas of other aspects.

The desertification situation in the arid region of the northern part of China is still very serious, and the areas in which it is obviously developing should be the focus of desertification control. The government can develop strict environmental protection regulations that, when combined with effective sand control and ecological protection measures, will improve the ecological environment of the entire region.

## ACKNOWLEDGEMENTS

The National Natural Science Foundation of China (4104011), High Performance Demonstration System of Earth Surface System for Scientific Research and Application (30-Y30B13-9003-14/16), The Fundamental Research Funds for the Central Universities (310827162026), and the Shaanxi Province Foundation of Important Science & Technology Innovative Team (No. 2016KCT-23) funded this work. We also appreciate sincerely Professor Li Sanzhong for providing much valuable advice about this paper.

## DISCLOSURE STATEMENT

There is no political bias in this paper.

## REFERENCES

- Armah, F. A., Odoi, J. O., Yengoh, G. T., Obiri, S., Yawson, D. O., & Afrifa, E. K. (2011). Food security and climate change in drought-sensitive savanna zones of Ghana. *Mitigation and Adaptation Strategies for Global Change*, 16, 291–306.
- Badreldin, N., & Goossens, R. (2013). A satellite-based disturbance index algorithm for monitoring mitigation strategies effects on desertification change in an arid environment. *Mitigation and Adaptation Strategies for Global Change*, 20, 263–276.
- Bai, Y. (2013). Study On Vegetation Coverage Change of Hulunbeier Sand Land By Remote Sensing. Inner Mongolia Agricultural University.
- Barzani, M. M., & Khairulmaini, O. (2013). Desertification risk mapping of the Zayandeh Rood Basin in Iran. *Journal of Earth System Science*, 122, 1269–1282.
- Cicchetti, D. V., & Feinstein, A. R. (1990). High agreement but low kappa: II. Resolving the paradoxes. *Journal of Clinical Epidemiology*, 43, 551–558.
- Cohen, J. (1968). Weighted kappa: Nominal scale agreement provision for scaled disagreement or partial credit. *Psychological Bulletin*, 70, 213.
- Dawelbait, M., & Morari, F. (2012). Monitoring desertification in a savannah region in Sudan using Landsat images and spectral mixture analysis. *Journal of Arid Environments*, 80, 45–55.
- Duan, H. C., Wang, T., Xue, X., Xun, J. H., & Hai, Y. L. (2013). Spatial-temporal evolution of aeolian desertification in the Horqin Sandy Land based on RS and GIS. *Journal of Desert Research*, 33, 470–477. (in Chinese with English abstract)
- Eswaran, H., Lal, R., & Reich, P. F. (2001). Land degradation: An overview. *Responses to Land degradation*, 20–35.
- Fang, Z. M., Yue, T. X., Chen, C. F., & Sun, X. F. (2011). Spatial change trends of temperature and precipitation in China. *Journal of Geo-Information Science*, 13, 526–533. (in Chinese with English abstract)
- Feinstein, A. R., & Cicchetti, D. V. (1990). High agreement but low kappa: I. The problems of two paradoxes. *Journal of Clinical Epidemiology*, 43, 543–549.
- Friedl, M. A., & Brodley, C. E. (1997). Decision tree classification of land cover from remotely sensed data. *Remote Sensing of Environment*, 61, 399–409.
- Gan, F. P., Wang, R. S., Wang, Y. J., & Fu, Z. W. (1999). The classification method based on remote sensing techniques for land use and cover. *Remote Sensing for Land & Resources*, 4, 40–45. (in Chinese with English abstract)
- Holm, A. M., Cridland, S. W., & Roderick, M. L. (2003). The use of time-integrated NOAA NDVI data and rainfall to assess landscape degradation in the arid shrubland of Western Australia. *Remote Sensing of Environment*, 85, 145–158.
- Hu, G. Y., Dong, Z. B., Lu, J. F., Song, X., & Zhenhai, W. (2010). Desertification land survey in source region of Yangtze River and analysis of its distribution characteristics. *Journal of Desert Research*, 30, 505–509. (in Chinese with English abstract)
- Hu, G. Y., Dong, Z. B., Lu, J. F., & Yan, C. Z. (2011). Spatial and temporal changes of desertification land and its influence factors in source region of the Yellow River from 1975 to 2005. *Journal of Desert Research*, 1079–1086. (in Chinese with English abstract)
- Hu, Y. N., He, W. L., Zhang, G. S., Qin, Y., Yin, W., & Peilin, Z. (2013). Wavelet analysis on the temporal series of principal climate factors in Mu Us Sandy Land during 1969–2009. *Journal of Desert Research*, 33, 390–395. (in Chinese with English abstract)
- Jia, S. H., Han, Z. G., Lv, M. N., Wang, J., & Dongqi, X. (2011). Extraction of desertification information based on decision tree in northern Liaoning province. *Ecology and Environmental Sciences*, 20, 13–18. (in Chinese with English abstract)
- Kang, W. P., Liu, S. L., & Duan, H. C. (2016). Monitoring and spatial-temporal changes analysis of aeolian desertified lands based on MODIS data. *Journal of Desert Research*, 36, 307–318. (in Chinese with English abstract)
- Li, A. M., Han, Z. W., Xu, J., Ma, S. X., & Huang, C. h. (2006). Transformation dynamics of desertification in Horqin Sandy Land at the beginning of the 21st century. *Acta Geographica Sinica*, 61, 976–984. (in Chinese with English abstract)
- Li, C. L., Meng, C. L., Bao, Y. H., & Yin, S. (2015a). Dynamic changes of desertification in the Hunshandake desert under the climate fluctuation in early 21st century. *Arid Land Geography*, 556–564. (in Chinese with English abstract)
- Li, C. Z., Liu, Z. H., & Yuan, L. (2011a). Analysis of dynamic changes of sandy desertification in the lower reaches of Tarim River based on decision tree classification. *Research of Environmental Sciences*, 933–941. (in Chinese with English abstract)
- Li, F., Zhao, J., Zhao, C. Y., & Zhang, X. Q. (2011b). Succession of potential vegetation in arid and semi-arid area of China. *Acta Ecologica Sinica*, 31, 689–697. (in Chinese with English abstract)
- Li, P. Y., Qian, H., Ken, W., Howard, F., & Wu, J. H. (2015b). Building a new and sustainable “Silk Road Economic Belt”. *Environmental Earth Sciences*, 74, 7267. (in Chinese with English abstract)
- Li, X. W., Zhang, L., Guo, H. D., Fu, W. X., Lu, L. L., Bao, Q. Y., ... Jia, G. S. (2016). Space recognition of eco-environment global change response of arid and semi-arid region of the Silk Road Economic Belt. *Bulletin of the Chinese Academy of Sciences*, 559–566. (in Chinese with English abstract)
- Li, Z. H., Wang, J. L., Zhao, Z. P., Dong, S. C., Yu, L., Yunqiang, Z., & Hao, C. (2014). Eco-environment patterns and ecological civilization modes in the Silk Road Economic Zone. *Resources Science*, 36, 2476–2482. (in Chinese with English abstract)
- Liu, H. M., Xun, B., Dong, X. B., & Zhang, X. S. (2010). The problems of water resource and corresponding measures caused by climate change and glacier melt in Xinjiang. *Ecological Economy*, 2, 176–178. (in Chinese with English abstract)
- Luo, J., Xu, D. Y., & Ren, H. Y. (2013). The desertification dynamics in Ordos from 2000 to 2010 and their relationship with climate change and human activities. *Journal of Glaciology and Geocryology*, 35, 48–56. (in Chinese with English abstract)

- Ma, Y. F., Sha, Z. J., Niu, Z. N., Guo, L. H., Zhang, X. L., & Zhang, H. C. (2010). Spatial autocorrelation analysis on sandy landscape pattern in the peripheral regions of the Qinghai Lake. *Arid Zone Research*, 27, 954–961. (in Chinese with English abstract)
- Meng, X. C., Jiang, Q. G., Qi, X., Wang, B., Wu, Y. C., Li, G. J., & Yang, J. (2012). Extraction of desertification information in Hulun Buir based on MODIS image data. *Journal of Anhui Agricultural Science*, 40, 2977–2979. (in Chinese with English abstract)
- Millennium Ecosystem Assessment Council. (2005). *Ecosystems and Human Well-being: Desertification Synthesis* (pp. 1–22). Washington, DC: World Resources Institute.
- Nicholson, S. E., Tucker, C. J., & Ba, M. (1998). Desertification, drought, and surface vegetation: An example from the West African Sahel. *Bulletin of the American Meteorological Society*, 79, 815–829.
- Reiche, M., Funk, R., Zhang, Z., Hoffmann, C., Reiche, J., Wehrhan, M., ... Sommer, M. (2012). Application of satellite remote sensing for mapping wind erosion risk and dust emission-deposition in Inner Mongolia grassland, China. *Grassland Science*, 58, 8–19.
- Ren, H. J., & Tang, J. (2015). Strategy study of the integrated ecological protection of the Silk Road Economic Belt. *Journal of Lanzhou University (Social Sciences)*, 53–61. (in Chinese with English abstract)
- Reynolds, J. F., Grainger, A., Stafford Smith, D. M., Bastin, G., Garcia-Barrros, L., Fernández, R. J., ... Zdruli, P. (2011). Scientific concepts for an integrated analysis of desertification. *Land Degradation & Development*, 22, 166–183.
- Sastry, G. S., Ganesha Raj, K., Paul, M. A., Dhinwa, P. S., & Sastry, K. L. N. (2016). Desertification vulnerability assessment model for a resource rich region: A case study of Bellary District, Karnataka, India. *Journal of the Indian Society of Remote Sensing*, 1–13.
- Schaaf, C. B., Gao, F., Strahler, A. H., Lucht, W., Li, X., Tsang, T., ... Muller, J.-P. (2002). First operational BRDF, albedo nadir reflectance products from MODIS. *Remote Sensing of Environment*, 83, 135–148.
- Sepehr, A., Hassanli, A. M., Ekhtesasi, M. R., & Jamali, J. B. (2007). Quantitative assessment of desertification in south of Iran using MEDALUS method. *Environmental Monitoring and Assessment*, 134, 243.
- Sobrino, J., El Kharraz, J., & Li, Z.-L. (2003). Surface temperature and water vapour retrieval from MODIS data. *International Journal of Remote Sensing*, 24, 5161–5182.
- Sun, B., Liu, Y., & Lei, Y. (2016). Growing season relative humidity variations and possible impacts on Hulunbuir grassland. *Science Bulletin*, 61, 728–736.
- Tottrup, C., & Rasmussen, M. S. (2004). Mapping long-term changes in savannah crop productivity in Senegal through trend analysis of time series of remote sensing data. *Agriculture, Ecosystems & Environment*, 103, 545–560.
- Tracy, E. F., Shvarts, E., Simonov, E., & Babenko, M. (2017). China's new Eurasian ambitions: The environmental risks of the Silk Road Economic Belt. *Eurasian Geography and Economics*, 58, 56–88.
- Tu, Z. F., Li, M. X., & Sun, T. (2016). The status and trend analysis of desertification and sandification. *Forest Resources Management*, 1, 1–5. (in Chinese with English abstract)
- Tucker, C. J., Pinzon, J. E., Brown, M. E., Slayback, D. A., Pak, E. W., Mahoney, R., ... El Saleous, N. (2005). An extended AVHRR 8-km NDVI dataset compatible with MODIS and SPOT vegetation NDVI data. *International Journal of Remote Sensing*, 26, 4485–4498.
- Türkeş, M. (1999). Vulnerability of Turkey to desertification with respect to precipitation and aridity conditions. *Turkish Journal of Engineering and Environmental Sciences*, 23, 363–380.
- Vogt, J., Safriel, U., Von Maltitz, G., Sokona, Y., Zougmore, R., Bastin, G., & Hill, J. (2011). Monitoring and assessment of land degradation and desertification: Towards new conceptual and integrated approaches. *Land Degradation & Development*, 22, 150–165.
- Wang, J. F., & Xu, C. D. (2017). Geodetector: Principle and prospective. *Acta Geographica Sinica*, 72, 116–134.
- Wang, T., Song, X., Yan, C. Z., Li, S., & Jiali, X. (2011). Remote sensing analysis on aeolian desertification trends in northern China during 1975–2010. *Journal of Desert Research*, 31, 1351–1356. (in Chinese with English abstract)
- Wang, T., Zhu, Z. D., & Wu, W. (2002). Sandy desertification in the north of China. *Science in China Series D: Earth Sciences*, 45, 23–34. (in Chinese with English abstract)
- Wang, X. F., Reng, Z. Y., & Ma, Z. M. (2009). Study on desertification dynamics along the great wall by GIS and RS. *Journal of Desert Research*, 29, 623–627. (in Chinese with English abstract)
- Wang, Y. F., Zhang, J. Q., Ma, Q. Y., & Zhu, M. (2016). Response of aeolian desertification to regional climate change in Horqin Sandy Land at beginning of 21st century. *Transactions of the Chinese Society of Agricultural Engineering*, 177–185. (in Chinese with English abstract)
- Yao, J. Q., Yang, Q., Cheng, Y. N., Hu, W. F., Liu, Z. H., & Zhao, L. (2013). Climate change in arid areas of Northwest China in past 50 years and its effects on the local ecological environment. *Chinese Journal of Ecology*, 32, 1283–1291. (in Chinese with English abstract)
- Zeng, Y. N., Xiang, N. P., Feng, Z., & Xu, H. (2006). Albedo-NDVI space and remote sensing synthesis index models for desertification monitoring. *Scientia Geographica Sinica*, 26, 75–81. (in Chinese with English abstract)
- Zhu, H. Y., & Li, X. B. (2003). Discussion on the index method of regional land use change. *Acta Geographica Sinica*, 58, 643–650. (in Chinese with English abstract)
- Zolotokrylin, A., Gunin, P., Titkova, T., Bazha, S., Danzhalova, E., & Kazantseva, T. (2016). Diagnosis of the desertification dynamics of arid pastures in Mongolia from observation in key areas and MODIS data. *Arid Ecosystems*, 6, 149–157.

**How to cite this article:** Wang X, Yin L, Xiao F, et al. The desertification process in the Silk Road Economic Belt in the past 15 years: A study using MODIS data and GIS analysis. *Geological Journal*. 2018;53(S1):322–331. <https://doi.org/10.1002/gj.2986>